A Detailed Examination of a Single Conduction Event in a Potassium Channel – Supplementary Information

Philip W. Fowler, Oliver Beckstein[*]*, Enrique Abad*[†] *and Mark S. P. Sansom*[‡]
Department of Biochemistry, University of Oxford, South Parks Rd, Oxford, OX1 3QU

Supplementary Discussion

In such a complex computational study it is important to be mindful of any potential shortcomings. We have assumed that the process of conduction can be described classically, which may not be true given the high electric field inside the selectivity filter. The prevailing view is that two ions and two waters alternate in single-file in the selectivity filter (the KwK mechanism). To produce the above mechanism we therefore assumed, like most other studies, that the selectivity filter is populated by an alternating series of ions and water molecules[1]. Since intervening waters can escape from the selectivity filter, this suggests that other mechanisms in addition to KwK are possible. This effect has been seen in unbiased simulations of Kv1.2 by Jensen *et al.*[2]. It has also been suggested that mechanisms involving vacancies (e.g. KK) are possible[3]. The 3-ion KwKwK configuration has been repeatedly shown to be more stable than either of the 2-ion configurations[4], indicating that a 4-ion mechanism may play a role, as previously suggested[5]. The first structure of a potassium ion channel only predicted the existence of sites S1-4[6], hence the KwKwK configuration was not studied in early theoretical studies[7]. Despite running three sets of umbrella simulations we were unable to calculate three independent PMFs since we had to aggregate the data following the removal of frames where the KwK mechanism did not hold. This is unfortunate, since comparing independent repeats of PMFs allows one to better estimate the error. Although the sampling, both in terms of the region of (z_{12}, z_3) space covered and the durations of the umbrella sampling simulations, is improved compared to our earlier work, it may still be insufficient[4]. Finally, the voltage sensors of Kvchim were not included and these could have an effect of the free energy landscape potassium ions and water molecules experience as they move through the selectivity filter.

Computational Details

Construction and equilibration of the simulation unit cell

The simulation unit cell containing the central pore domain of the Kv paddle chimaera[8] was constructed, its energy minimised and its temperature increased as described elsewhere[9]. Briefly, potassium ions were placed in the cavity of the channel and at the S4, S2 and S0 positions with intervening waters placed at the S1 and S3 positions. The cavity of the pore was filled with water molecules using the voidoo and flood[10] programs. The CHARMM27 forcefield with the CMAP correction was used[11] and therefore all hydrogens are included and water is described using the TIP3P model. The interac-

[*]Current address: Department of Physics, Arizona State University, USA
[†]Current address: Departamento de Física Aplicada, Centro Universitario de Mérida, Universidad de Extremadura, Mérida, Spain
[‡]mark.sansom@bioch.ox.ac.uk

tions between carbonyl oxygens and potassiums was modified to better reproduce the free energy in liquid N-methylacetylamide[12]. The simulation unit cell had a total of 72 354 atoms.

These and all subsequent molecular dynamics simulations were run using NAMD2.7[13] in the NpAT ensemble. The pressure was maintained at 1 atm using a Langevin Piston barostat with a period of 200 fs and a decay time of 100 fs[14,15]. The temperature was maintained at 310K by a Langevin thermostat with a damping coefficient of 1.0 ps^{-1}. SHAKE and SETTLE were applied to constrain the length of all bonds that involve a hydrogen allowing an integration timestep of 2 fs[16,17]. Electrostatic forces were calculated every 4 fs using the particle mesh Ewald method[18] with a grid spacing of 1 Å and van der Waals forces were truncated at 12 Å with a switching function applied from 10 Å. The channel was equilibrated for 10 ns in the NpAT ensemble during which time the filter remained in the KwKwK configuration.

Structures of the filter in two additional states were created by swapping ions and waters as done previously[3,19]; one in each of the wwKwK(K) and wKwKw(K) configurations. The collective variables for the umbrella sampling were defined in the same way as a previous study[20]; the top and bottom of the selectivity filter is defined as the centres of mass of the backbone atoms of TV (residues 370 & 371) and GY (residues 372 & 373). The unit vector between these points defines the pore axis, z. The displacement of each ion or water is therefore simply the projection onto this axis using linear algebra. The three potassium ions are labelled 1–3 starting from the extracellular side (Fig. 1). We defined two collective variables: the projected centre of mass of the two potassium ions in the filter (z_{12}) and the projection of the third potassium ion (z_3). We then used umbrella sampling and by applying harmonic potentials with spring constants of 40.0 and 20.0 kcal/mol/Å^2 to z_{12} and z_3 were able to map out a region of (z_{12}, z_3) space corresponding to a single conduction event. To ensure efficient sampling a trigonal pattern of restraint points was used where each point is 0.5 Å equidistant from its six neighbouring points. A total of 125 umbrellas, each 500 ps long, was run from each of the three independent starting structures yielding 375 umbrellas in total. Starting an umbrella simulation where the ions are a long way from the centres of their biasing harmonic potentials leads to large initial forces which can distort the selectivity filter. To prevent this we capped the magnitude of the biasing force during the first 10 ps of each umbrella simulation. The caps were set at 15 and 7.5 kcal/mol/Å for z_{12} and z_3, respectively. In unbiased simulations of K channels, one of the four Val372 residues (or its equivalent), occasionally 'flips' such that one carbonyl oxygen now points away from the pore axis[21]. When this occurs, the filter becomes trapped in this conformation. We assume that this does not represent a conductive state and therefore applied a half-harmonic potential with a spring constant of 80 kcal/mol/rad^2 when the ψ dihedral angle of Val371 becomes larger than 20° or smaller than -20°.

All of the above was coded using the Tclforces module of NAMD which permits on-the-fly calculation and application of bespoke forces. This also allowed us to record the positions of the ions every 20 fs, the coordinates of the selectivity filter and intervening waters every 200 fs whilst the coordinates of the entire system was stored every 10 ps. Frequently storing the coordinates of a subset of the atoms was crucial as it allowed us to investigate in detail how the geometry of the filter changes during a conduction event.

Checking that the KwK mechanism is maintained

Each of the 375 umbrella simulations was parsed to determine if an alternating single file of potassium ions and waters is maintained throughout all simulations. The numbers of waters between ion1 and ion2 (n_{12}) and ion2 and ion3 (n_{23}) were counted. The latter was only done if ion3 had entered the filter which was defined as its z-coordinate (pore coordinate) being greater than (i.e. above) the z-coordinate of the centre of mass of the hydroxyl oxygens of Thr370 which form the bottom half of S4. Then all frames in the trajectories where either n_{12} or n_{23} were not equal to one were discarded (Table S1). The dihedral angles of Val371 were also analysed to see if any had 'flipped', thereby reducing the coordination number in sites S2 and S3. As expected this did not occur due to the imposition of a half-harmonic potential as mentioned above.

Convergence and error analysis of the 2D PMF

All the remaining umbrella simulations were combined. This aggregated dataset was divided into 250 bins, each 2 ps wide. The biases were removed using the Weighted Histogram Analysis Method (WHAM)[22], producing a series of 250 correlated 2D PMFs (Fig. S2A). We used the WHAM implementation written by Alan Grossfield[23]. The minimum free energy path (MFEP) across each 2D PMF was found using the nudged elastic band (NEB) method as described elsewhere[24]. We implemented our own NEB method in python, including many of the improvements suggested by the authors (for example keeping some component of the velocity between successive steps). The variation of the free energy along the MFEP was characterised by three energies (Fig. S2B & C). Following the ideas of Yang *et al.*[25], we calculated the statistical inefficiency, s.[26,27]. Suppose we have N correlated datapoints with a known variance, $\sigma^2(x)$. One first divides the data into a series of blocks, each of length n, and the mean of each block is calculated. The variance of these means, $\sigma^2(y)$, is then calculated as a function of n. The statistical inefficiency, s, is defined as

$$s = \lim_{n\to\infty} \frac{n\sigma^2(y)}{\sigma^2(x)} \tag{1}$$

One can either plot s v n or s v $n^{1/2}$ and determine what s is tending towards as n tends to infinity. The error in the mean in then given by

$$\sigma^2(\bar{x}) = \frac{s\sigma^2(x)}{N} \tag{2}$$

The statistical inefficiency as a function of the reverse penetration into the three free energy datasets (Fig. S2D & E) suggests that (1) we should discard the first ~20% of the dataset to avoid equilibration artefacts and (2) the correlation time for the remaining 400 ps is 5–10 ps. We were conservative and used a larger correlation time of 20 ps. The remaining data were then divided into 20 bins, each 20 ps wide, and a PMF calculated for each (Fig. S3). These independent PMFs were then averaged and the error estimated in the usual way (Fig. S4).

Alchemical free energy calculations

Two independent structures were chosen from the umbrella simulations; one in the KwKwK configuration and the other in the wwKwK(K) configuration. In the former a water in the cavity was

swapped with the potassium ion at site S0 (Fig. S5). For the latter this process was reversed. A parameter, λ, was defined that measured the degree of alchemical decoupling. In both cases twenty-one equally-spaced λ values ($\lambda = 0.00, 0.05, 0.10 \ldots 1.00$) were run, each for 300 ps, using the NAMD colvars module. A soft-core van der Waals potential with a shifting radius of 5 Å was used and the electrostatics and van der Waals were separately decoupled. The energies were written to disc every 20 ps. All other parameters are the same as above.

We divided both sets of data into bins 4 ps wide and calculated 7,500 correlated values of ΔG. Examining how the statistical inefficiency changed (see above) as differing amounts of data were discarded (Fig. S5) suggested that the simulations are equilibrated after the first 120 ps and 5 ps is a conservative estimate of the correlation time.

Structural analysis

All structural analysis was performed using a python script that used the numpy and MDAnalysis modules[28] to read in simulation trajectories and measure distances etc. This built upon GridDataFormats, another python module written by Oliver Beckstein[29]. All graphs were plotted using gnuplot and all images rendered using VMD[30].

description	proportion
fail KwK	8.0% (8.8%)
fail $\psi < 0$	none
data remaining	88.4%

Table S1: The single file KwK assumption is broken in 8% of the frames (8.8% of the time when all ions are inside the filter). These data are removed from all subsequent analysis. A half-harmonic restraint was applied at all times to the ψ backbone angle of Val-371 and this prevented any carbonyl flips. For practical reasons we discarded the remainder of each umbrella simulation as soon as the single file assumption breaks. We therefore removed 11.6% of the total umbrella simulation data.

Label	Description	Free energy (kcal/mol)	(z_{12}, z_3) coordinate
1	wwKwK(K)	4.0 ± 0.5	(-1.8, -12.3)
2	possible intermediate	5.4 ± 0.4	(-1.8, -9.2)
3	barrier height	7.5 ± 0.5	(-1.3, -8.3)
4	possible intermediate	3.4 ± 0.3	(-0.1, -7.4)
5	wKwK(K)	1.4 ± 0.2	(1.6, -7.0)
6	barrier height	8.0 ± 0.1	(3.0, -6.9)
7	possible intermediate	4.1 ± 0.2	(4.1, -6.8)
8	KwKwK	0.0 ± 0.1	(4.3, -5.2)
9	part of barrier height	5.9 ± 0.5	(4.3, -4.1)

Table S2: The values of the free energy and the (z_{12}, z_3) coordinates (Å) of the nine labelled points in Fig. 2.

$\Delta G^{\ddagger}_{1\to5}$	$\Delta G^{\ddagger}_{5\to1}$	$\Delta G^{\ddagger}_{5\to8}$	$\Delta G^{\ddagger}_{8\to5}$	$\Delta G_{8\to1}$	$\Delta G_{8\to5}$
3.5 ±0.6	6.1 ±0.5	6.5 ±0.2	7.9 ±0.1	4.0 ±0.5	1.4 ±0.2

Table S3: The heights (kcal/mol) of the forward and reverse barriers between the identified states. For comparison $5kT$ = 3 kcal/mol. For a definition of the barrier heights, e.g. $\Delta G^{\ddagger}_{1\to5}$, see Fig. S4C

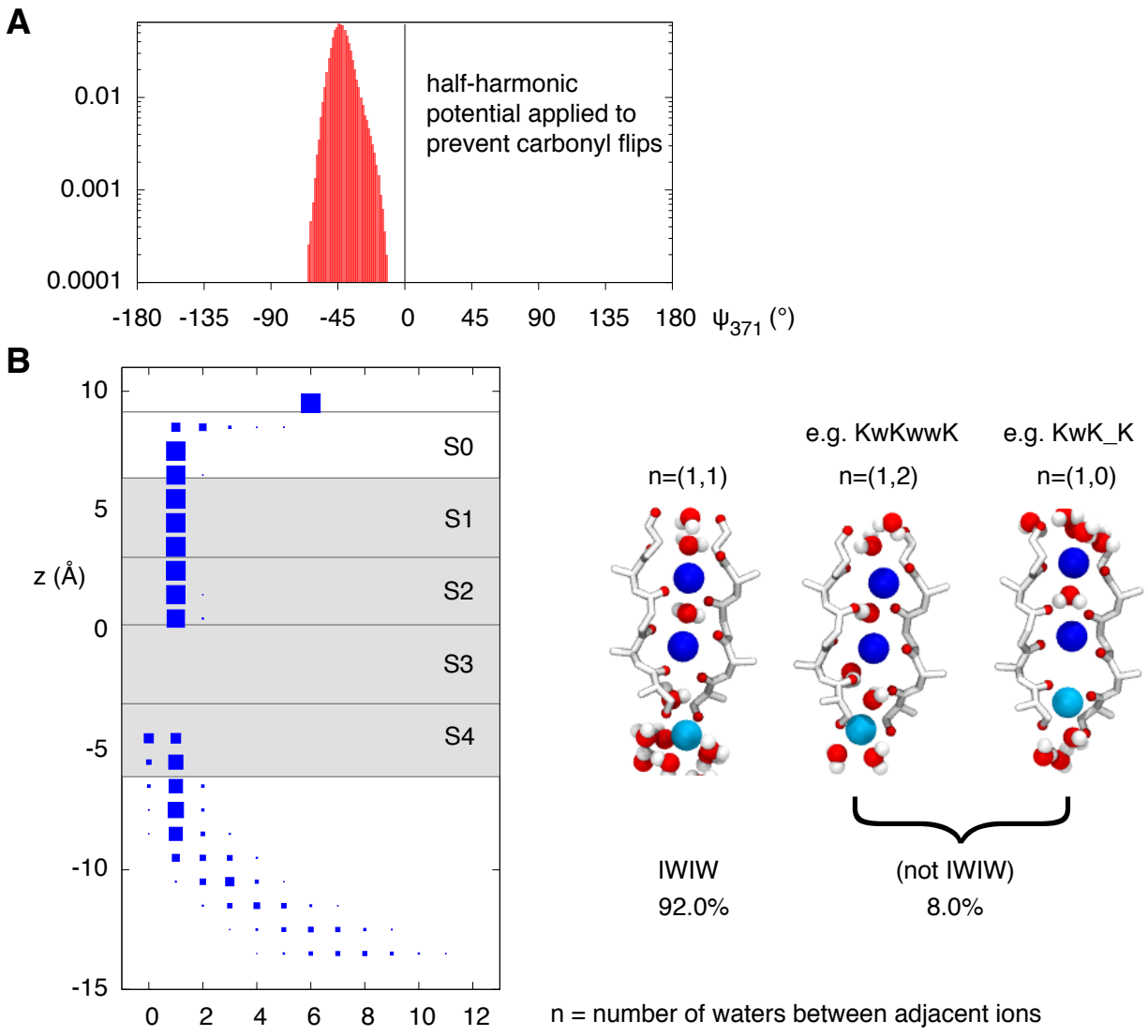

Figure S1: **A** We applied a half-harmonic restraint to the ψ angle of Val-371 to keep the filter in a conductive state. As shown by this log histogram, $\psi < 0°$ for all umbrella simulations. **B** The number of waters between adjacent ions is plotted as a function of the z coordinate of the ion furthest from the center of the selectivity filter. The area of the blue squares on a row is proportional to its % occurrence. We define an ion to be 'inside' the selectivity filter if it is within sites S1-S4. This is defined as the z coordinate is greater than the center of mass of the hydroxyl oxygens of Thr370 and less than center of mass of the carbonyl oxygens of Tyr373. This region is shaded grey. In most simulations when all three ions are inside the filter there is only one water between potassiums. In around 8% of all umbrella simulations there are 0, 2 or more waters between two of the potassiums. To ensure the KwK mechanism these frames were excluded from subsequent analysis[4].

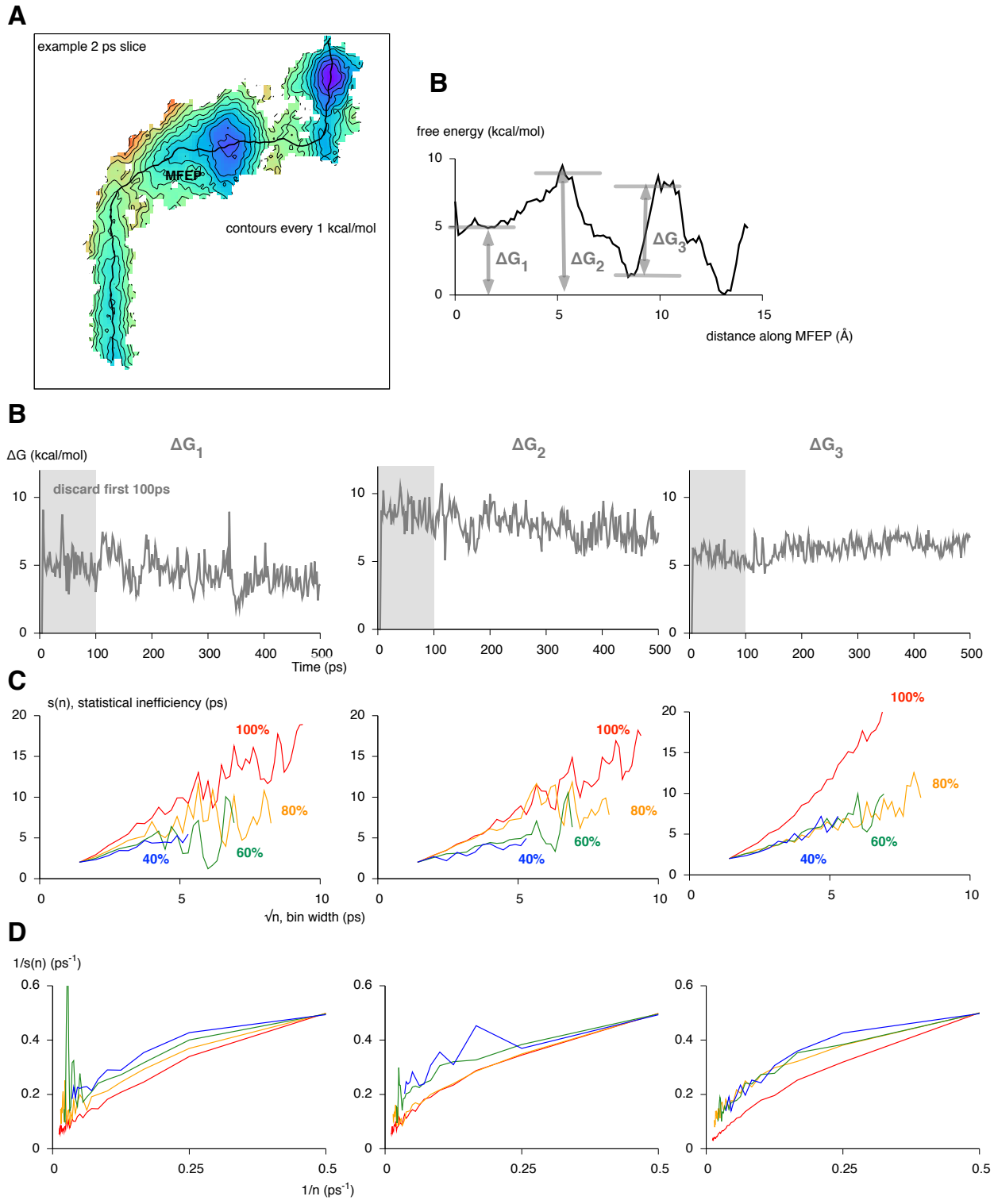

Figure S2: To estimate both when the data are equilibrated and the statistical error we divided each 500 ps umbrella simulation into 250 blocks of width 2 ps and the 2D PMF calculated as described elsewhere. **A** An example is shown here and the minimum free energy path (MFEP) is drawn on as a black line. Three free energies were then extracted from the resulting 1D PMF as shown. **B** Examining how these vary with time illustrates that there is at least an initial equilibration period. To better understand this data the statistical inefficiency, $s(n)$, was then calculated as a function of the bin width, n. Plotting **C** $s(n)$ against $\sqrt{n}$ and **D** $1/s(n)$ against $1/n$ suggests that $\sim$20% of the data should be discarded and the correlation time is $5-10$ps. We shall therefore discard the first 20% (100ps) of all data and assume a correlation time of 20 ps.

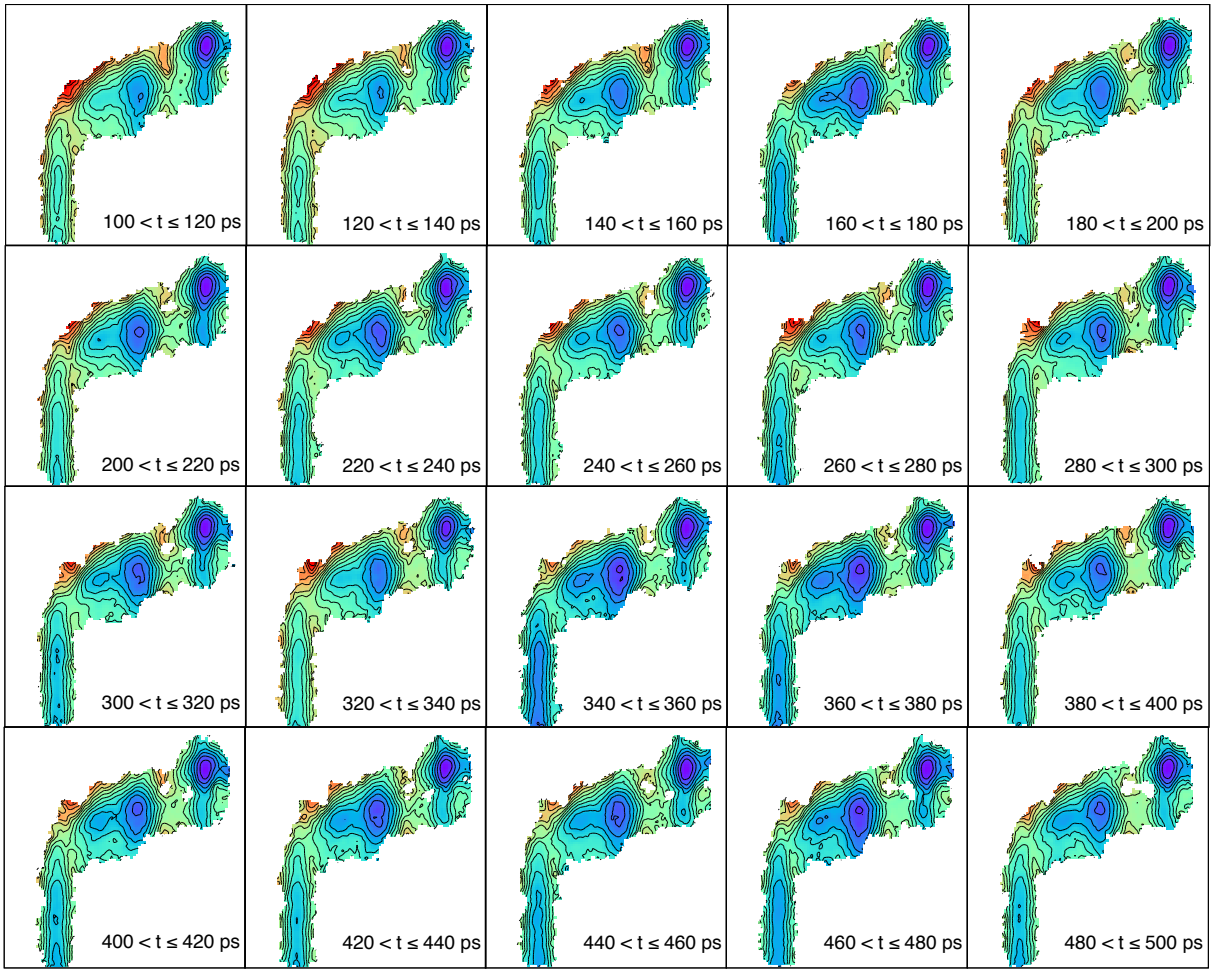

Figure S3: Using these estimates (Fig. S2) We can therefore calculate 20 independent 2D PMFs (if we discard the first 100 ps of all data and use a correlation time of 20 ps). These are plotted on the same scale and with the same colouring and contouring as in Fig. 2A.

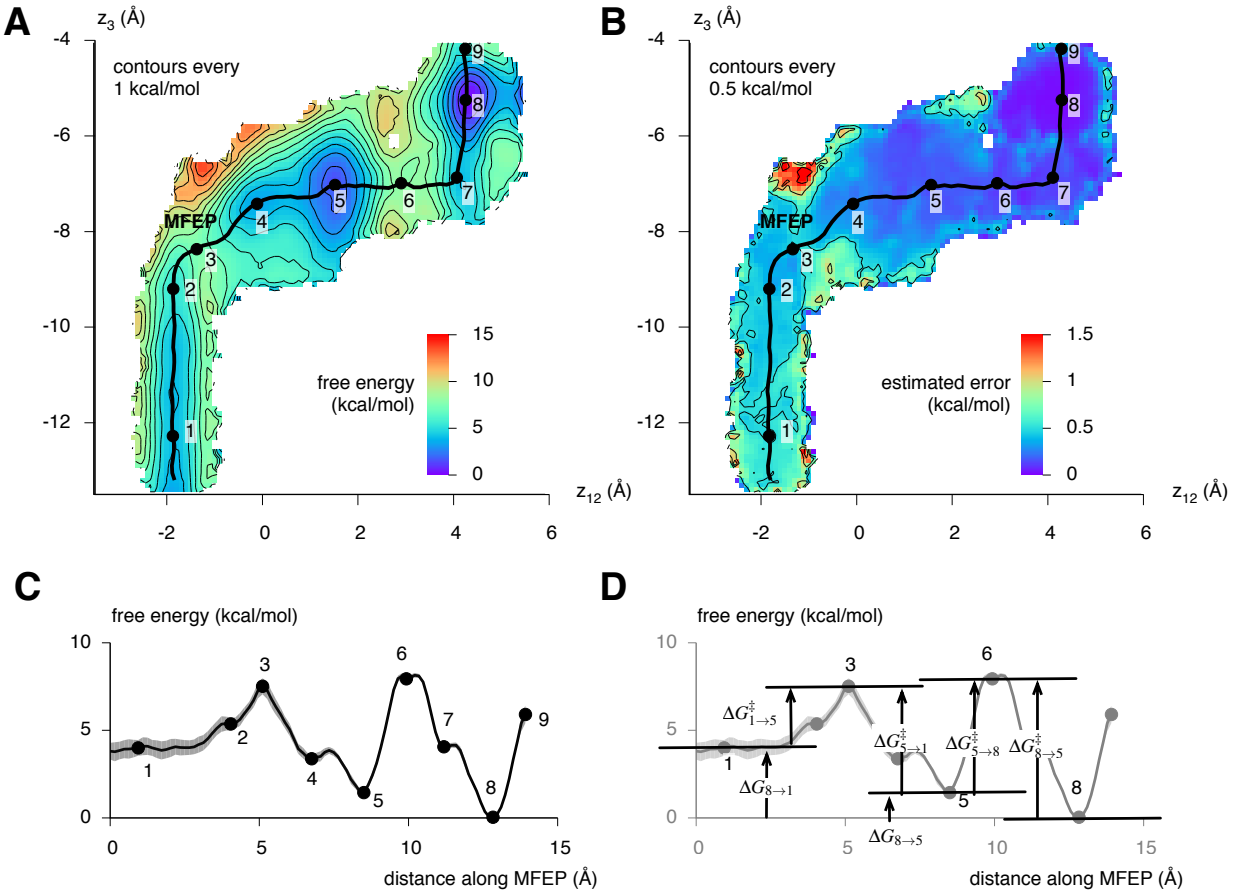

Figure S4: These PMFs (Fig. S3) are then combined, yielding **A** the final average result and **B** an estimate of the statistical error. The nudged elastic band method is used to calculate the minimum free energy path (MFEP) across the final 2D PMF and we can then plot **C** how the free energy varies along this path. This includes the estimate for the standard error which is less than 0.5 kcal/mol along the entire MFEP. **D** We define the energetic barriers between different stable configurations as shown. The subscripts refer to the starting and finishing states, respectively.

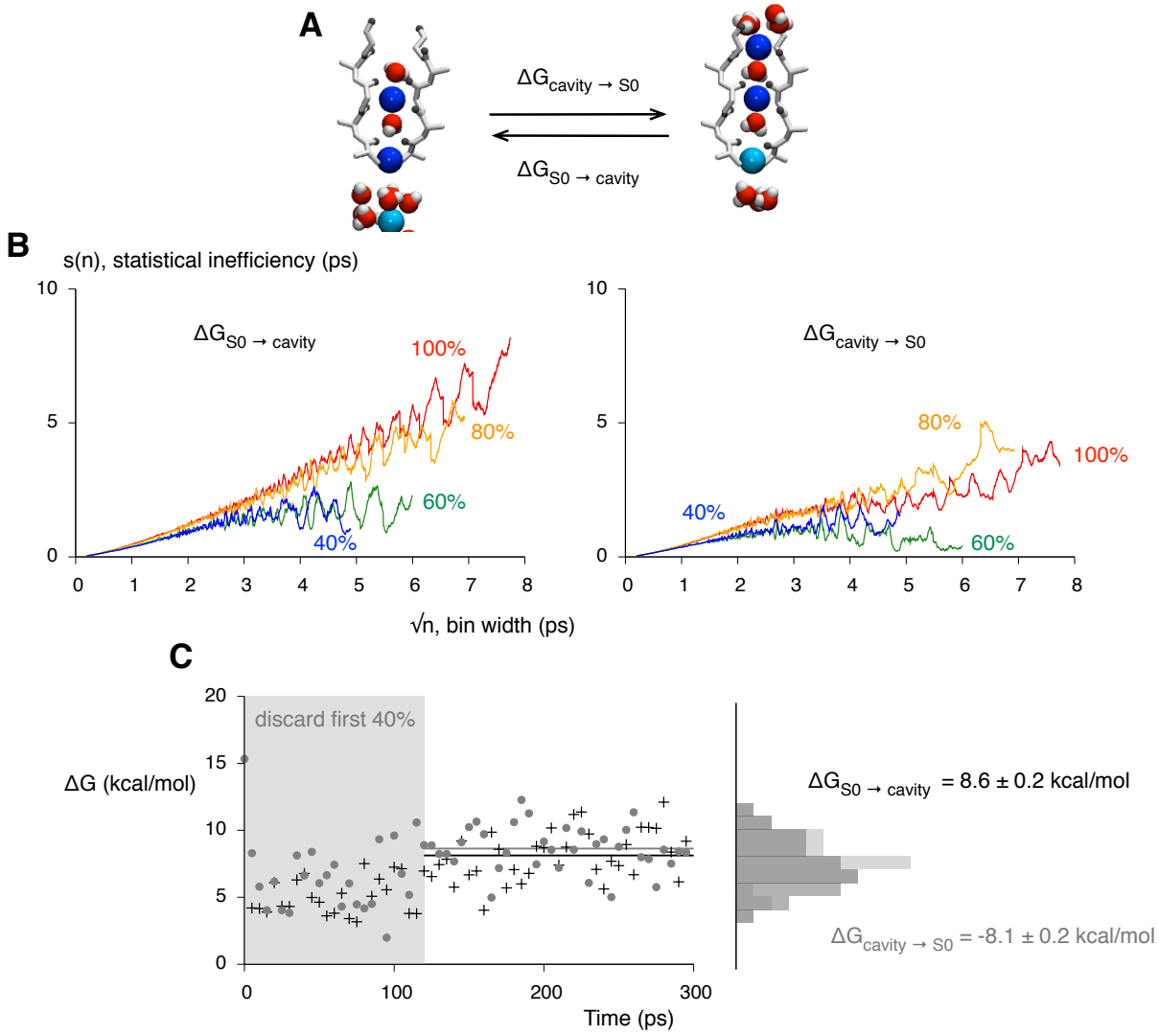

Figure S5: As an independent check of the final result **A** the free energies required to move a potassium ion from the central cavity to S0 (and the opposite process) were calculated using thermodynamic integration. **B** The data from each λ simulation was divided into small blocks and the statistical inefficiency was calculated. This suggested that the first 40% should be discarded and we used a conservative estimate of 5 ps for the correlation time. **C** The free energy of moving a potassium ion from cavity to S0 was estimated to be 8.1 $\pm$ 0.2 kcal/mol. This is within error of the reverse process which was estimated to be -8.6 $\pm$ 0.2 kcal/mol. We can compare these values to those derived from the 2D PMF. The latter estimates a similar process to be 4.0 $\pm$ 0.5 kcal/mol (compare points 1 and 8 - see Fig S4).

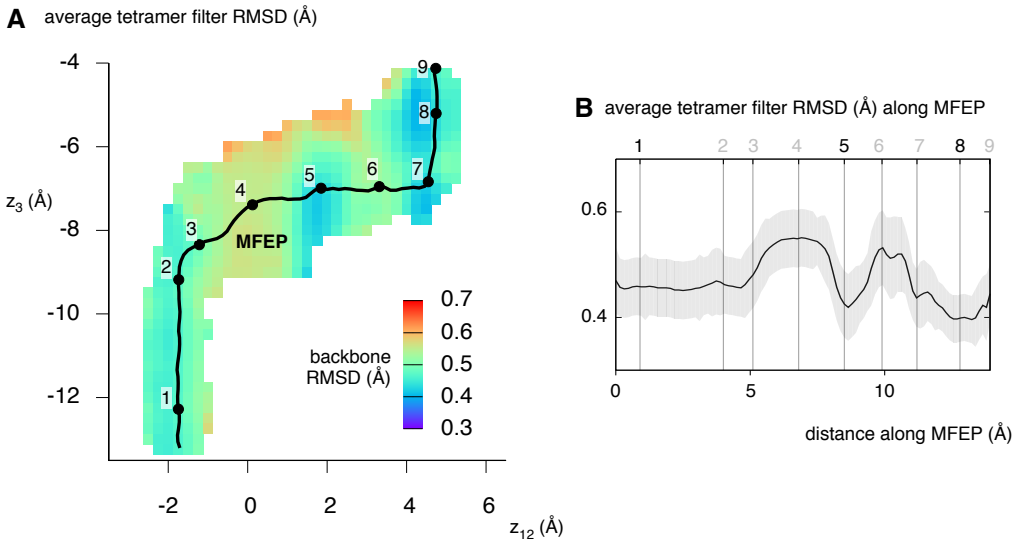

Figure S6: **A** The RMSD of the selectivity filter varies across the (z_{12}, z_3) region sampled. The MFEP is shown as before. **B** The variation along the MFEP shows how the selectivity filter is most similar to the crystal structure when ions and waters are stably bound (points 1, 5, 8) and of the three states, the KwKwK configuration is the most similar to the crystal structure. The RMSD is calculated relative to the crystal structure of Kvchim[8] and compares the backbone heavy atoms (C_α, C, N, O) as well as the C_β atoms of the entire selectivity filter (the sequence TVGYG).

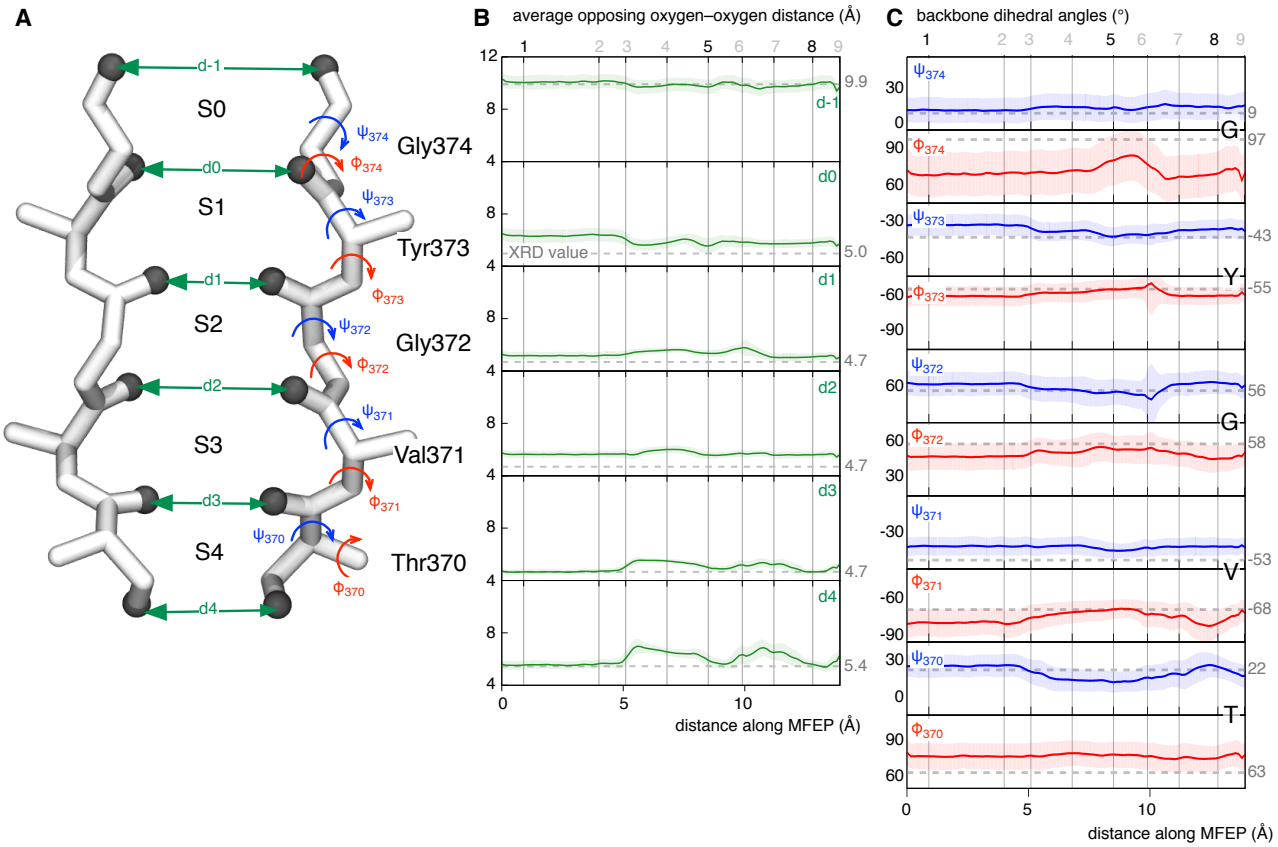

Figure S7: The selectivity filter changes conformation during the conduction event. **A** Definitions of the the backbone dihedral angles and the opposing oxygen distances[31]. **B** The former shows that the selectivity filter undergoes a motion reminiscent of peristalsis as ions move through the planes formed by the backbone carbonyl oxygens. This is most clearly seen for the hydroxyl sidechains of Thr370 (d4). When ion3 is several Angstroms below the filter the distance is the same as measured experimentally (the dotted grey line is the distance measured from the crystal structure), but as it approaches Thr370, d4 first increases to allow water23 to enter the filter as the species above are knocked on. In the stable wKwKw(K) configuration it again is similar to that seen in the crystal structure but then increases again by several Angstroms as ion3 enters the filter. The standard deviation is also drawn but is usually too small to be seen. **D** The average (ϕ, ψ) angles also vary significantly during a conduction event. Again a dotted grey line indicates the value taken in the crystal structure.

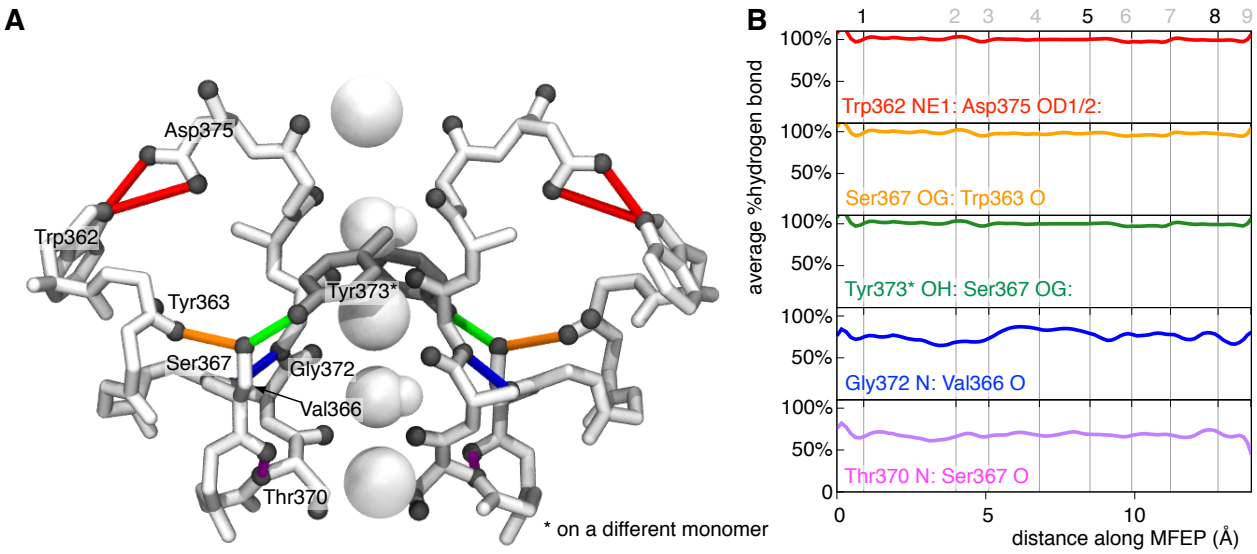

Figure S8: **A** There is a network of hydrogen bonds around the selectivity filter that help stabilise its structure. **B** Several of the hydrogen bonds (e.g. Ser367 OG: Trp363 O) are maintained throughout the conduction event whereas others (e.g. Gly372 N: Val 366 O) vary as the selectivity filter changes conformation to accommodate the varying numbers of ions and waters.

References

[1] Zhou, Y. and R. MacKinnon, 2003. The Occupancy of Ions in the K^+ Selectivity Filter: Charge Balance and Coupling of Ion Binding to a Protein Conformational Change Underlie High Conduction Rates. *J Mol Biol* 333(5):965–975. doi:10.1016/j.jmb.2003.09.022.

[2] Jensen, M. O., D. W. Borhani, K. Lindorff-Larsen, P. Maragakis, V. Jogini, M. P. Eastwood, R. O. Dror and D. E. Shaw, 2010. Principles of Conduction and Hydrophobic Gating in K^+ Channels. *Proc Natl Acad Sci U S A* 107(13):5833–8. doi:10.1073/pnas.0911691107.

[3] Furini, S. and C. Domene, 2009. Atypical Mechanism of Conduction in Potassium Channels. *Proc Natl Acad Sci U S A* 106(38):16 074–7. doi:10.1073/pnas.0903226106.

[4] Fowler, P. W., E. Abad, O. Beckstein and M. S. Sansom, 2013. Energetics of Multi-Ion Conduction Pathways in Potassium Ion Channels. *submitted to J Chem Theo Comp* .

[5] Furini, S. and C. Domene, 2011. Selectivity and Permeation of Alkali Metal Ions in K^+-Channels. *J Mol Biol* 409(5):867–78. doi:10.1016/j.jmb.2011.04.043.

[6] Doyle, D., J. Cabral, R. Pfuetzner, A. Kuo, J. M. Gulbis, S. L. Cohen, B. T. Chait and R. MacKinnon, 1998. The Structure of the Potassium Channel: Molecular Basis of K^+ Conduction and Selectivity. *Science* 280(5360):69–77. doi:10.1126/science.280.5360.69.

[7] Aqvist, J. and V. Luzhkov, 2000. Ion Permeation Mechanism of the Potassium Channel. *Nature* 404(6780):881–4. doi:10.1038/35009114.

[8] Long, S. B., X. Tao, E. B. Campbell and R. MacKinnon, 2007. Atomic Structure of a Voltage-Dependent K^+ Channel in a Lipid Membrane-Like Environment. *Nature* 450(7168):376–82. doi:10.1038/nature06265.

[9] Fowler, P. W. and M. S. P. Sansom, 2013. The Pore of Voltage-Gated Potassium Ion Channels Is Strained When Closed. *Nat Comms* 4:1872. doi:10.1038/ncomms2858.

[10] Kleywegt, G. J. and T. A. Jones, 1994. Detection, Delineation, Measurement and Display of Cavities in Macromolecular Structures. *Acta Cryst D* 50(Pt 2):178–85. doi:10.1107/S0907444993011333.

[11] Mackerell, A. D., 2004. Empirical Force Fields For Biological Macromolecules: Overview and Issues. *J Comp Chem* 25(13):1584–604. doi:10.1002/jcc.20082.

[12] Roux, B. and S. Bernèche, 2002. On the Potential Functions Used In Molecular Dynamics Simulations of Ion Channels. *Biophys J* 82(3):1681–4. doi:10.1016/S0006-3495(02)75520-3.

[13] Phillips, J. C., R. Braun, W. Wang, J. Gumbart, E. Tajkhorshid, E. Villa, C. Chipot, R. D. Skeel, L. Kalé and K. Schulten, 2005. Scalable Molecular Dynamics with NAMD. *J Comp Chem* 26(16):1781–802. doi:10.1002/jcc.20289.

[14] Martyna, G. J., D. J. Tobias and M. L. Klein, 1994. Constant Pressure Molecular Dynamics Algorithms. *J Chem Phys* 101(5):4177. doi:10.1063/1.467468.

[15] Feller, S. E., Y. Zhang, R. W. Pastor and B. R. Brooks, 1995. Constant Pressure Molecular Dynamics Simulation: The Langevin Piston Method. *J Chem Phys* 103(11):4613. doi:10.1063/1.470648.

[16] Ryckart, J., G. Ciccotti and H. Berendsen, 1977. Numerical Integration of the Cartesian Equations of Motion of a System With Constraints: Molecular Dynamics of n-Alkanes. *J Comp Phys* 23(3):327–341. doi:10.1016/0021-9991(77)90098-5.

[17] Miyamoto, S. and P. A. Kollman, 1992. Settle: An Analytical Version of the SHAKE and RATTLE Algorithm for Rigid water models. *J Comp Chem* 13(8):952–962. doi:10.1002/jcc.540130805.

[18] Darden, T., D. York and L. Pedersen, 1993. Particle Mesh Ewald: An N log(N) Method for Ewald Sums in Large Systems. *J Chem Phys* 98(12):10 089. doi:10.1063/1.464397.

[19] Furini, S. and C. Domene, 2011. Gating at the Selectivity Filter of Ion Channels that Conduct Na^+ and K^+ Ions. *Biophys J* 101(7):1623–31. doi:10.1016/j.bpj.2011.08.035.

[20] Bernèche, S. and B. Roux, 2001. Energetics of Ion Conduction through the K^+ Channel. *Nature* 414(6859):73–7. doi:10.1038/35102067.

[21] Bernèche, S. and B. Roux, 2005. A Gate in the Selectivity Filter of Potassium Channels. *Structure* 13(4):591–600. doi:10.1016/j.str.2004.12.019.

[22] Kumar, S., J. M. Rosenberg, D. Bouzida, R. H. Swendsen and P. A. Kollman, 1992. The Weighted Histogram Analysis Method for Free-Energy Calculations on Biomolecules. I. The Method. *J Comp Chem* 13(8):1011–1021. doi:10.1002/jcc.540130812.

[23] Grossfield, A., 2012. WHAM: The Weighted Histogram Analysis Method. Version 2. URL `http://membrane.urmc.rochester.edu/content/wham/`.

[24] Jónsson, H., G. Mills and K. W. Jacobsen, 1998. Nudged Elastic Band Method for Finding Minimum Energy Paths of Transitions. In *Classical and Quantum Dynamics in Condensed Phase Simulations - Proceedings of the International School of Physics*, chapter 16, pages 385–404. World Scientific Publishing Co. Pte. Ltd., Singapore. doi:10.1142/9789812839664_0016.

[25] Yang, W., R. Bitetti-Putzer and M. Karplus, 2004. Free Energy Simulations: Use of Reverse Cumulative Averaging to Determine the Equilibrated Region and the Time Required for Convergence. *J Chem Phys* 120(6):2618–28. doi:10.1063/1.1638996.

[26] Friedberg, R., 1970. Test of the Monte Carlo Method: Fast Simulation of a Small Ising Lattice. *J Chem Phys* 52(12):6049. doi:10.1063/1.1672907.

[27] Morales, J. J., M. J. Nuevo and L. F. Rull, 1990. Statistical Error Methods in Computer Simulations. *J Comp Phys* 89(2):432–438. doi:10.1016/0021-9991(90)90151-P.

[28] Michaud-Agrawal, N., E. J. Denning, T. B. Woolf and O. Beckstein, 2011. MDAnalysis: A Toolkit for the Analysis of Molecular Dynamics Simulations. *J Comp Chem* 32(10):2319–2327. doi:10.1002/jcc.21787.

[29] Beckstein, O., 2013. GridDataFormats. URL `https://github.com/orbeckst/GridDataFormats`.

[30] Humphrey, W., A. Dalke and K. Schulten, 1996. VMD: Visual Molecular Dynamics. *J Mol Graph* 14(1):33–8.

[31] Fowler, P. W., K. Tai and M. S. P. Sansom, 2008. The Selectivity of K^+ Ion Channels: Testing the Hypotheses. *Biophys J* 95(11):5062–72. doi:10.1529/biophysj.108.132035.